Inorganic Chemistry
Article

Inorg. Chem. **2010**, *49*, 4433–4439 **4433**
DOI: 10.1021/ic9018629

Mixed-Donor, α-Hydroxy Acid-Containing Chelates for Binding and Light-Triggered Release of Iron

Hannah Sayre,[†] Kyle Milos,[†] Michael J. Goldcamp,[‡] Cynthia A. Schroll,[†] Jeanette A. Krause,[†] and Michael J. Baldwin*,[†]

[†]*Department of Chemistry, University of Cincinnati, Cincinnati, Ohio 45221-0172, and* [‡]*Department of Chemistry, Wilmington College, Wilmington, Ohio 45177*

Received September 21, 2009

A series of five new α-hydroxy acid-containing chelates inspired by photoactive marine siderophores, along with their Fe(III) complexes, have been synthesized and characterized. These chelates, designated X-Sal-AHA, each contributes a bidentate salicylidene moiety (X-Sal, X = 5-NO_2, 3,5-diCl, H, 3,5-di-*tert*-butyl, or 3-OCH_3 on the phenolate ring) and a bidentate α-hydroxy acid moiety (AHA). The X-ray crystal structure of Na[Fe_3(3,5-diCl-Sal-AHA)$_3$(μ_3-OCH_3)] shows an Fe(III) trimer with the triply deprotonated, trianionic ligands each spanning two Fe(III)'s that are bridged by the hydroxyl group of the ligand. Additionally, a μ_3-methoxy anion caps the Fe(III)$_3$ face. Electrospray ionization mass spectra demonstrate that this structure is representative of the Fe(III) complexes of all five derivatives in methanol solution, with the exception of the X = 3,5-di-*t*-Bu derivative having a μ_3-OH bridge rather than a methoxy bridge. Stability constants determined from reduction potentials range from 10^{34} for the 5-NO_2 derivative to >10^{40} for the 3,5-di-*t*Bu derivative. All five complexes are photoactive when irradiated by sunlight, with the relative rate of photolysis as monitored by Fe(II) transfer correlating with the Hammett σ^+ parameter for the phenolate ring substituents.

Introduction

To sequester iron, bacteria biosynthesize molecules called siderophores that bind Fe(III) very strongly. In a number of marine bacteria, the iron is rendered bioavailable to the bacteria as Fe(II) by a photochemical reaction that reduces the iron while cleaving the siderophore.[1−6] These photochemically active siderophores all have an α-hydroxy acid-related functional group among their iron-coordinating groups. An α-hydroxy acid (carboxylate form) to Fe(III) charge transfer transition is the chromophore responsible for the photolysis reaction.[7]

The Fe(III) complexes of much simpler α-hydroxy acid (AHA)-containing polycarboxylates like citrate and tartrate undergo similar photolysis reactions.[8,9] These simple chelates are oxygen-only donors coordinating the α-hydroxy group and varying numbers of carboxylates. Some polycarboxylates and aminopolycarboxylates that lack the α-hydroxy group, including EDTA, form photoactive Fe(III) complexes as well. However, with the exception of oxalate with its adjacent carboxylates, their quantum yields are much lower than those of the AHA-containing polycarboxylate complexes.[8−12] Few structurally characterized metal complexes of either natural product[13−15] or synthetic[16,17] mixed-donor chelates of intermediate complexity that incorporate an AHA group have been reported. A search of the literature reveals a lack of studies on the effect of systematically varying the

*To whom correspondence should be addressed. E-mail: michael.baldwin@uc.edu.

(1) Barbeau, K.; Rue, E. L.; Bruland, K. W.; Butler, A. *Nature* **2001**, *413*, 409–413.
(2) Barbeau, K.; Zhang, G.; Live, D. H.; Butler, A. *J. Am. Chem. Soc.* **2002**, *124*, 378–379.
(3) Holt, P. D.; Reid, R. R.; Lewis, B. L.; Luther, G. W., III; Butler, A. *Inorg. Chem.* **2005**, *44*, 7671–7677.
(4) Kupper, F. C.; Carrano, C. J.; Kuhn, J.-U.; Butler, A. *Inorg. Chem.* **2006**, *45*, 6028–6033.
(5) Martin, J. D.; Ito, Y.; Homann, V. V.; Haygood, M. G.; Butler, A. *J. Biol. Inorg. Chem.* **2006**, *11*, 633–641.
(6) Amin, S. A.; Green, D. H.; Kupper, F. C.; Carrano, C. J. *Inorg. Chem.* **2009**, *48*, 11451–11458.
(7) Barbeau, K.; Rue, E. L.; Trick, C. G.; Bruland, K. W.; Butler, A. *Limnol. Oceanogr.* **2003**, *48*, 1069–1078.
(8) Abrahamson, H. B.; Rezvani, A. B.; Brushmiller, J. G. *Inorg. Chim. Acta* **1994**, *226*, 117–127.
(9) Faust, B. C.; Zepp, R. G. *Environ. Sci. Technol.* **1993**, *27*, 2517–2522.
(10) Carey, J. H.; Langford, C. H. *Can. J. Chem.* **1973**, *51*, 3665–3670.
(11) Svenson, A.; Kaj, L.; Bjorndal, H. *Chemosphere* **1989**, *18*, 1805–1808.
(12) Kocot, P.; Karocki, A.; Stasicka, Z. *J. Photochem. Photobiol. A* **2006**, *179*, 176–183.
(13) Mino, Y.; Ishida, T.; Ota, N.; Inoue, M.; Nomoto, K.; Yoshioka, H.; Takemoto, T.; Sugiura, Y.; Tanaka, H. *Inorg. Chem.* **1981**, *20*, 3440–3444.
(14) Okabe, N.; Adachi, Y. *Acta Crystallogr.* **1999**, *C55*, 302–304.
(15) Odoko, M.; Adachi, Y.; Okabe, N. *Acta Crystallogr.* **2002**, *E58*, m7–m9.
(16) Ng, C. H.; Chong, T. S.; Teoh, S. G.; Ng, S. W. *J. Coord. Chem.* **2005**, *58*, 1455–1461.
(17) Angus, P. M.; Golding, B. T.; Jurisson, S. S.; Sargeson, A. M.; Willis, A. C. *Aust. J. Chem.* **1994**, *47*, 501–510.

Published on Web 04/16/2010

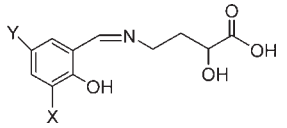

Figure 1. Generalized structure of the X-Sal-AHA series of chelates (neutral form). Derivatives reported here include X = H, Y = NO_2; X = Y = Cl; X = Y = H; X = OCH_3, Y = H; X = Y = *tert*-Bu. The chelates are prepared as the Na^+-carboxylate salts. When coordinated to Fe(III), all three of the protons shown in the drawing dissociate.

ancillary (non-AHA) functional groups in AHA-containing chelates on the photochemical properties of their metal complexes.

Synthetic molecules, inspired by the marine siderophores, that are designed to tightly bind Fe(III) and then to release the iron when irradiated by light of the appropriate wavelength are anticipated to have a number of useful applications including photodynamic metallopharmaceuticals, light-triggered molecular devices, or light-activated coatings. We have begun investigating a series of new AHA-containing chelate complexes with differing ligand structural and electronic features. The motivation of these studies is to control various aspects of metal binding and photochemistry to design application-specific properties into these stimulus-responsive molecules.

An alternative strategy that has been reported for the design of chelates that are sensitive to photocleavage is to append nitrophenyl groups to the backbone, thus providing molecules that "cage" Ca^{2+}[18,19] and other metal ions[20] and release them upon irradiation. Recently, Franz and co-workers have applied this approach for the first time to a biologically important d-block metal with the light-activated release of caged Cu^{2+},[21] and Burdette and co-workers have applied it to Zn^{2+}.[22] The work here complements these earlier studies; the AHA chelates differ from the nitrophenyl-appended chelates in that the AHA chelates are not photoactive themselves, but become photoactive only upon metal coordination.

Here, we present the synthesis, structural characterization, and initial photochemical experiments for the first series of systematically varied, AHA-containing chelates and their iron complexes. The generalized chelate structure is shown in Figure 1. It includes a terminal, bidentate α-hydroxy acid group as well as the imine and phenolate donor groups of a salicylidene moiety. The only variable in this series of chelates is the electron-richness of the phenolate as determined by electron-donating or -withdrawing ring substituents. This allows analysis of the effects of the electron donor ability of ancillary functional groups on the photochemistry, without the complication of significant structural differences. These studies provide the "proof-of-concept" for predictable synthetic control of photochemical properties of mixed-donor, AHA-containing metal-bound chelates through straightforward modification of the ancillary donor groups. They also demonstrate the potential of the AHA group incorporated into polydentate ligands to promote formation of small metal clusters with high stability constants.

Experimental Section

Syntheses. All chemicals were obtained from either Fisher/Acros or Aldrich and used without further purification.

Chelating Ligands, NaH_2(X-Sal-AHA). All five ligands were prepared similarly. The synthesis for NaH_2(3,5-diCl-Sal-AHA) is given, with differences in the syntheses of other derivatives noted: 0.95 g (3 mmol) of (*S*)-(-)-4-amino-2-hydroxybutyric acid (see Supporting Information for crystallographic details) was dissolved in 5 mL of distilled water. A 0.37 g portion (3 mmol) of $NaHCO_3$ and 0.18 g (3 mmol) of NaCl were added to the solution. Separately, 0.58 g (3 mmol) of 3,5-dichlorosalicylaldehyde was dissolved in 65 mL of methanol and added dropwise to the aqueous solution. (For other derivatives, the amount of methanol necessary to dissolve the salicylaldehyde derivative varied. Unsubstituted salicylaldehyde is a liquid and was added neat. For the 5-NO_2 derivative, the water was first removed by rotary evaporation from the hydroxybutyric acid solution, and the resulting residue was redissolved in methanol with the 5-NO_2-salicylaldehyde.) The solution turned from clear to bright yellow and was stirred, covered, overnight. The solvent was removed by rotary evaporation. The resulting solid was extracted with methanol, filtered to remove residual salts, and the methanol was removed by rotary evaporation. Yields ranged from 50 to 90% depending on the derivative. ^{1}H NMR spectra (CD_3OD, ppm): X = 3,5-diCl-Sal-AHA, 2.01 (m, 1H), 2.17 (m, 1H), 2.82 (t, 2H), 4.02 (t, 1H), 7.26 (s, 1H), 7.45 (s, 1H), 8.43 (s, 1H); X = 5-NO_2, 2.02 (m, 1H), 2.19 (m, 1H), 3.84 (t, 2H), 4.00 (m, 1H), 6.66 (d, 1H), 8.11 (d, 1H), 8.37 (s, 1H), 8.57 (s, 1H); X = H, 1.92 (m, 1H), 2.10 (m, 1H), 3.71 (t, 2H), 3.95 (t, 1H), 6.75 (overlapping d's, 2H), 7.24 (t, 2H), 8.40 (s, 1H) + starting material impurity peaks @ 1.8, 2.9, 3.9; X = 3,5-di*t*Bu, 1.28 (s, 9H), 1.40 (s, 9H), 1.93 (m, 1H), 2.15 (m, 1H), 3.73 (t, 2H), 4.01 (t, 1H), 7.15 (s, 1H), 7.34 (s, 1H), 8.44 (s, 1H); X = 3-OCH_3, 1.96 (m, 1H), 2.15 (m, 1H), 3.81 (s + t, 5H), 3.99 (t, 1H), 6.59 (t, 1H), 6.89 (m, 2H), 8.39 (s, 1H).

Fe(III) Complexes of X-Sal-AHA Ligands. The Fe(III) complexes of all five ligand derivatives were prepared similarly. The synthesis of Na[Fe_3(3,5-diCl-Sal-AHA)$_3$(μ_3-OCH_3)] is given: 120 mg (0.5 mmol) of NaH_2(3,5-diCl-Sal-AHA) was dissolved in 30 mL of methanol. A 84 mg portion (1 mmol) of $NaHCO_3$ was added to the stirring solution. A 30 mL methanolic solution/slurry containing 60 mg (approximately 0.25 mmol) of $Fe_2(SO_4)_3 \cdot xH_2O$ was added to the ligand solution. The solution (red-orange to purple, depending on ligand derivative) was stirred overnight, wrapped in foil to prevent light exposure. Solvent was removed by rotary evaporation. The product was recrystallized by slow evaporation of a methanol solution in the dark. Yields ranged from 15 to 40%, depending on the ligand derivative. Electrospray ionization mass spectra (negative ion mode): [Fe_3(3,5-diCl-Sal-AHA)$_3$(OCH_3)]$^-$, 1064.84 (obs.), 1064.77 (calc.); [Fe_3(Sal-AHA)$_3$(OCH_3)]$^-$, 859.12 (obs.), 859.01 (calc.); [Fe_3(3-OCH_3-Sal-AHA)$_3$(OCH_3)]$^-$, 949.08 (obs.), 949.06 (calc.); [Fe_3(3,5-di*t*Bu-Sal-AHA)$_3$(OH)]$^-$, 1181.09 (obs.), 1181 (calc.); [Fe_3(5-NO_2-Sal-AHA)$_3$(OCH_3)]$^-$, 993.95 (obs.), 993.96 (calc.). In all cases, the M^- peak given is the dominant peak above the free ligand mass (see Supporting Information).

Instrumental Methods. All of the experiments described were done for methanol solutions; although the presence of water does not appear to adversely affect the complexes or their photochemistry, the complexes are insufficiently soluble in water to provide satisfactory results. Electrospray ionization mass spectra were collected at the University of Cincinnati Mass Spectrometry Facility on an IonSpec 4.7 T ESI-FTMS spectrometer.

(18) Adams, S. R.; Kao, J. P. Y.; Grynkiewicz, G.; Minta, A.; Tsien, R. Y. *J. Am. Chem. Soc.* **1988**, *110*, 3212–3220.
(19) Kaplan, J. H.; Ellis-Davies, G. C. R. *Proc. Natl. Acad. Sci. U.S.A.* **1988**, *85*, 6571–6575.
(20) Kishimoto, T.; Liu, T.-T.; Ninomiya, Y.; Takagi, H.; Yoshioka, T.; Ellis-Davies, G. C. R.; Miyashita, Y.; Kasai, H. *J. Physiology* **2001**, *533*, 627–637.
(21) Ciesienski, K. L.; Haas, K. L.; Dickens, M. G.; Tesema, Y. T.; Franz, K. J. *J. Am. Chem. Soc.* **2008**, *130*, 12246–12247.
(22) Bandara, H. M. D.; Kennedy, D. P.; Akin, E.; Incarvito, C. D.; Burdette, S. C. *Inorg. Chem.* **2009**, *48*, 8445–8455.

NMR spectra were obtained on a Bruker AC 250 MHz NMR spectrometer. UV/visible absorption spectra were obtained with a Spectral Instruments Model 420 fiber optic dip probe spectrophotometer. Circular dichroism spectra were obtained with a JASCO 751 CD spectrophotometer. Cyclic voltammograms for 0.5 mM solutions of the Fe(III) trimers in methanol with 0.1 M $NaClO_4$ were obtained on a BAS 50W electrochemical analyzer using an aqueous Ag/AgCl reference electrode, glassy carbon working electrode, and Pt auxiliary electrode. The reference electrode was soaked in a saturated aqueous KCl solution between samples to maintain hydration of the membrane. Little difference is observed for scan rates ranging from 10 mV/s to 1000 mV/s; data are presented for scan rates of 25 mV/s. Under these conditions, the ferrocene/ferrocinium couple is observed at $E_{1/2}$ = 417 mV with ΔE = 70 mV.

Photolysis Experiments. In photolysis experiments reported here, samples were irradiated by direct sunlight; irradiation by a high-intensity Hg lamp gives similar results. In experiments comparing multiple Fe(III) complexes or conditions, solutions in Type I, Class B borosilicate glass vials were irradiated side-by-side in direct sunlight, spaced sufficiently to prevent shading of samples. Independent samples were prepared for each time point, and the samples were wrapped in aluminum foil upon completion of the irradiation period to avoid further light exposure. Fe(II) production was measured spectrophotometrically by measuring the absorbance at 535 nm from the chromophore produced by coordination of bathophenanthroline disulfonate (BPDS) to Fe(II), as applied by Butler and coworkers to the siderophore aquachelin.[1] Methanol solutions for data shown in which Fe(II) production was monitored at time points of 30 min or less were 60 μM in complex (180 μM in Fe) and 200 μM in BPDS to optimize the spectra, while data reported for longer times used solutions that were 20 μM in complex (60 μM in Fe) and 200 μM in BPDS to ensure sufficient BPDS to form $Fe(BPDS)_3^{2+}$ with 100% of the Fe present, unless otherwise noted. All experiments were performed under both conditions.

X-ray Crystallography. Single crystals of $Na[Fe_3(3,5\text{-diCl-Sal-AHA})_3(\mu_3\text{-}OCH_3)]\cdot 3.5\ H_2O$ were obtained as dark red plates from methanol. For X-ray examination and data collection, a suitable crystal, approximate dimensions 0.17 × 0.12 × 0.08 mm, was mounted in a loop with Paratone-N oil and transferred to the goniostat bathed in a cold stream. Intensity data were collected at 120 K out to 62° in θ on a Bruker SMART6000 CCD diffractometer using graphite-monochromated Cu Kα radiation, λ = 1.54178 Å. The data frames were processed using the program SAINT.[23] The data were corrected for decay, Lorentz and polarization effects as well as absorption and beam corrections based on the multiscan technique.[24] The structure was solved by a combination of direct methods in SHELXTL[24] and the difference Fourier technique and refined by full-matrix least-squares on F^2. Non-hydrogen atoms were refined with anisotropic displacement parameters with the exception of the disordered carbon atoms. Two of the dichlorophenyl rings are disordered; a reasonable two-component model is presented. Waters of crystallization (3.5 molecules) are present in the lattice. One of these water molecules is disordered over two positions set at 50% occupancy. The H-atoms were either located or calculated; water H atoms were held fixed while the others were treated with a riding model. The H-atom isotropic displacement parameters were defined as aU_{eq} of the adjacent atom (a = 1.5 for −OH and $-CH_3$ and 1.2 for all others). The refinement converged with crystallographic agreement factors as listed in Table 1.

(23) Sheldrick, G. M. *SAINT*, v7.46A; Bruker Analytical X-ray Instruments, Inc.: Madison, WI.

(24) Sheldrick, G. M. *SADABS*, v2007/4; Bruker Analytical X-ray Instruments, Inc.: Madison, WI.

Table 1. Crystallographic Parameters and Data and Refinement Information for $Na[Fe_3(3,5\text{-diCl-Sal-AHA})_3(\mu_3\text{-}OCH_3)]\cdot 3.5H_2O$

empirical formula	$Na[(C_{11}H_8NO_4Cl_2Fe)_3(OCH_3)]\cdot 3.5H_2O$
formula weight	1151.88
temperature	120(2) K
wavelength	1.54178 Å
crystal system	monoclinic
space group	C_2
unit cell dimensions	a = 18.2256(5) Å b = 10.9468(3) Å c = 23.2182(7) Å α = 90° β = 101.337(1)° γ = 90°
volume, Z	4541.9(2) Å^3, 4
index ranges	$-20 \le h \le 20$ $-12 \le k \le 12$ $-26 \le l \le 26$
reflections collected, independent reflections	17163, 6971 (R_{int} = 0.0653)
data/restraints/parameters	6971/5/593
Final R indices [$I > 2\sigma(I)$]	R1 = 0.0549, wR2 = 0.1207
R indices (all data)	R1 = 0.758, wR2 = 0.1287

Results and Discussion

The bright yellow salicylidene/α-hydroxy acid compounds designated X-Sal-AHA shown above in Figure 1 result from the Schiff base condensation of the primary amine of the chiral compound (*S*)-(-)-4-amino-2-hydroxybutyric acid with a series of salicylaldehyde derivatives. This condensation reaction requires an equivalent of base, such as $NaHCO_3$, to deprotonate the amine nitrogen of the zwitterionic amino acid starting material. The 5-NO_2-Sal-AHA, 3,5-diCl-Sal-AHA, 3-OCH_3-Sal-AHA, 3,5-di-*tert*-Bu-Sal-AHA, and Sal-AHA products are thus formed as the sodium carboxylate salts. In the unsubstituted Sal-AHA case, there appears to be an equilibrium between starting materials and chelate product with loss of some of the volatile salicylaldehyde. This results in the 4-amino-2-hydroxybutyric acid impurities in the NMR spectrum of Sal-AHA. This is not observed for the other chelates since the substituted salicylaldehydes are solids with very low volatility. Even in the Sal-AHA case, though, clean Fe(III) complexes [vide infra] are obtained.

Reaction of the Na(X-Sal-AHA$^-$) chelates with ferric sulfate in methanol results in orange to purple solutions. The Fe(III) complex of 3,5-diCl-Sal-AHA produces X-ray quality crystals as deep red plates from methanol. Although the Fe(III) complex forms with a 1:1 Fe/L ratio, it has a trimeric rather than monomeric structure. The complex crystallizes in the monoclinic C_2 space group as the sodium salt of a trimeric monoanion, $Na[Fe_3(3,5\text{-diCl-Sal-AHA})_3(\mu_3\text{-}OCH_3)]\cdot 3.5\ H_2O$ (see Table 2 and Figure 2). The carboxylate, hydroxyl, and phenolate groups are all deprotonated to give the trianionic ligand, countering the +3 charge of the Fe. The negative charge of the anion is due to a methoxy group that symmetrically caps the Fe(III) face. The structure of the anion can be described as consisting of an Fe_3O_4 iron-oxo cubane core with one corner missing. Three Sal-AHA ligands fold upward forming a basket with the three phenyl rings, anchored to the iron atoms via three μ_2-alkoxo bridges arising from the hydroxyl groups of the ligands. The methoxy anion forms the fourth oxygen corner of the Fe_3O_4 unit with the methyl group approximately centered in the phenyl basket. The carboxylate associated with each bridging

alkoxo coordinates to one of the bridged irons, while the phenolate and imine of the same ligand coordinate to the other iron. This trimeric structural motif likely forms to avoid the seven-member −N−C−C−C−C−O−Fe− chelate ring that would be necessary in a monomeric complex with the imine group and the carboxylate coordinated to the same iron. In the trimeric structure with each ligand spanning two irons, only the more stable 5- and 6-member chelate rings are required. The cavity depth of the basket is 6.9 Å from the centroid of the upper chlorine atoms (Cl1, Cl3, Cl5) to the Fe_3 core. The average non-bonded Fe−Fe distance is 3.265 Å. The average of the three $Fe-O_{methoxy}$ distances is 2.160 Å.

Table 2. Selected Crystallographically-Determined Distances (Å) and Angles (deg) from $Na[Fe_3(3,5\text{-diCl-Sal-AHA})_3(\mu_3\text{-}OCH_3)]\cdot 3.5H_2O$

Fe(1)···Fe(2)	3.2549(14)	Fe(1)···Fe(3)	3.2743(14)
Fe(2)···Fe(3)	3.2661(16)		
Fe(1)−O(11)	1.934(5)	Fe(1)−O(10)	1.960(4)
Fe(1)−O(1)	1.989(4)	Fe(1)−O(2)	1.998(4)
Fe(1)−N(3)	2.148(6)	Fe(1)−O(13)	2.151(4)
Fe(2)−O(2)	1.952(4)	Fe(2)−O(3)	1.938(5)
Fe(2)−O(6)	2.003(5)	Fe(2)−O(5)	1.998(5)
Fe(2)−N(1)	2.139(6)	Fe(2)−O(13)	2.168(5)
Fe(3)−O(6)	1.984(5)	Fe(3)−O(7)	1.936(5)
Fe(3)−O(9)	1.993(5)	Fe(3)−O(10)	2.004(4)
Fe(3)−N(2)	2.132(6)	Fe(3)−O(13)	2.162(5)
O(11)−Fe(1)−O(10)	157.5(2)	O(11)−Fe(1)−O(1)	97.9(2)
O(10)−Fe(1)−O(1)	102.47(19)	O(11)−Fe(1)−O(2)	98.5(2)
O(10)−Fe(1)−O(2)	94.39(19)	O(1)−Fe(1)−O(2)	79.44(18)
O(11)−Fe(1)−N(3)	85.5(2)	O(10)−Fe(1)−N(3)	84.0(2)
O(1)−Fe(1)−N(3)	93.4(2)	O(2)−Fe(1)−N(3)	172.2(2)
O(11)−Fe(1)−O(13)	90.09(19)	O(10)−Fe(1)−O(13)	75.48(18)
O(1)−Fe(1)−O(13)	154.43(19)	O(2)−Fe(1)−O(13)	75.35(18)
N(3)−Fe(1)−O(13)	111.5(2)	O(3)−Fe(2)−O(2)	155.2(2)
O(3)−Fe(2)−O(5)	98.2(2)	O(2)−Fe(2)−O(5)	103.9(2)
O(3)−Fe(2)−O(6)	98.7(2)	O(2)−Fe(2)−O(6)	96.8(2)
O(5)−Fe(2)−O(6)	78.2(2)	O(3)−Fe(2)−N(1)	85.1(2)
O(2)−Fe(2)−N(1)	83.5(2)	O(5)−Fe(2)−N(1)	90.8(2)
O(6)−Fe(2)−N(1)	168.7(2)	O(3)−Fe(2)−O(13)	89.29(19)
O(2)−Fe(2)−O(13)	75.87(18)	O(5)−Fe(2)−O(13)	153.7(2)
O(6)−Fe(2)−O(13)	75.77(19)	N(1)−Fe(2)−O(13)	115.0(2)
O(7)−Fe(3)−O(6)	159.2(2)	O(7)−Fe(3)−O(9)	96.8(2)
O(6)−Fe(3)−O(9)	101.5(2)	O(7)−Fe(3)−O(10)	98.54(19)
O(6)−Fe(3)−O(10)	94.41(19)	O(9)−Fe(3)−O(10)	79.22(19)
O(7)−Fe(3)−N(2)	84.6(2)	O(6)−Fe(3)−N(2)	84.4(2)
O(9)−Fe(3)−N(2)	94.5(2)	O(10)−Fe(3)−N(2)	173.2(2)
O(7)−Fe(3)−O(13)	91.59(19)	O(6)−Fe(3)−O(13)	76.30(19)
O(9)−Fe(3)−O(13)	153.17(19)	O(10)−Fe(3)−O(13)	74.35(16)
N(2)−Fe(3)−O(13)	111.7(2)	Fe(2)−O(2)−Fe(1)	111.0(2)
Fe(3)−O(6)−Fe(2)	110.0(2)	Fe(1)−O(10)−Fe(3)	111.4(2)
Fe(1)−O(13)−Fe(3)	98.78(18)	Fe(1)−O(13)−Fe(2)	97.81(18)
Fe(3)−O(13)−Fe(2)	97.93(18)		

The average of the three $Fe-O_{hydroxy}$ distances with the Fe coordinated to the carboxylate group associated with the bridging hydroxyl is 2.002 Å, while the average of the three with the iron coordinated to the associated salicylidene is 1.965 Å. Additional distances and angles are listed in Table 2.

Electrospray ionization mass spectra (ESI-MS) of methanol solutions of the Fe(III) complexes of all five X-Sal-AHA derivatives show that the trimeric structure observed for the anion in the crystal structure of $Na[Fe_3(3,5\text{-diCl-Sal-AHA})_3(\mu_3\text{-}OCH_3)]$ is consistent with the dominant species in solution (see Supporting Information). In negative ion mode, the X = 3,5-diCl, 5-NO_2, H, and 3-OCH_3 derivatives show a single feature in the m/z range above that of the free ligand corresponding to $[Fe_3L_3(OCH_3)]^-$. The major feature in the X = 3,5-di*t*-Bu derivative corresponds to $[Fe_3L_3(OH)]^-$, and several peaks corresponding to lower m/z complexes with intensities < 10% of that of the major peak are observed. The positive ion mode spectra are more complicated than the negative ion mode spectra, dominated by dimeric and monomeric species in addition to trimers. This is likely due to loss of the μ-OCH_3 or μ-OH bridge upon protonation. The positive mode spectra also appear noisier under the same conditions, suggesting that the negative mode spectra are representative of the more concentrated species.

Cyclic voltammograms of the $[Fe_3(X\text{-Sal-AHA})_3(\mu_3\text{-}OR)]^-$ complexes in methanol are quasireversible, except for the X = 3,5-di-*t*Bu derivative which is irreversible [see Supplementary Information]. They give reduction potentials ($E_{1/2} = 1/2\,(E_c + E_a)$) from −300 mV (vs Ag/AgCl) to below −540 mV, depending on the phenolate ring substituents, as listed in Table 3. These potentials can be converted to stability constants for the complexes by manipulation of the Nernst equation and the empirical correlation between reduction potential and stability constants of a series of Fe(III) complexes according to the method of Taylor and

Table 3. Electrochemical Data and Stability Constants for the $[Fe_3(X\text{-Sal-AHA})_3(\mu_3\text{-OR})]^-$ Complexes

X	E_c (mV vs Ag/AgCl)	E_a (mV vs Ag/AgCl)	$E_{1/2}$ (mV vs Ag/AgCl)	log K_{ox}
5-NO_2	−308	−248	−278	34.0
3,5-di-Cl	−415	−345	−380	36.5
H	−565	−480	−523	40.0
3-OCH_3	−551	−489	−520	40.0
3,5-di-*t*Bu	−730	not observed		

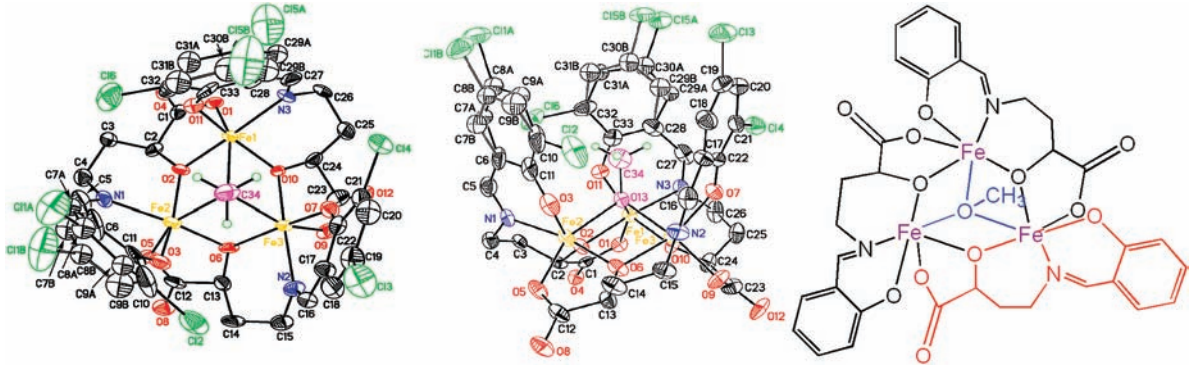

Figure 2. Two views of the ORTEP plot for the anion of $Na[Fe_3(3,5\text{-diCl-Sal-AHA})_3(\mu_3\text{-}OCH_3)]\cdot 3.5\ H_2O$. For clarity, only the methoxy H-atoms are shown. Both components of the disordered phenolate rings are shown. A line drawing (with ring Cl groups omitted) is shown on the right to clarify the arrangement of bonds in the trimer.

co-workers.[25] Taylor's "chelate scale" has been used by Butler and co-workers to determine the pH-independent stability constant for the Fe(III) complex of the AHA-containing siderophore, Alterobactin A.[3] The stability constants for the complexes presented here are given in Table 3, based on eq 1 derived from Taylor's work after a correction of 0.018 V to account for the difference in reference electrodes used. K_{ox} is the stability

$$\log K_{ox} = (1.10 - E_{1/2})/0.041 \qquad (1)$$

constant for the oxidized (Fe(III)) species in the redox couple. Values of log K_{ox} range from 34.0 for the X = 5-NO_2 derivative to 40.0 for the X = H and 3-OCH_3 derivatives. The value of log K_{ox} for the 3,5-di-*t*Bu derivative cannot be determined accurately because of the irreversibility of the electrochemistry, but is likely greater than 40 based on the observed cathodic potential. These stability constants are much higher than those of Fe(III) complexes of the simpler α-hydroxy polycarboxylates citrate and tartrate (log K = 11.5 and 12.3, respectively)[26] and the amino polycarboxylates NTA and EDTA (log K = 15.9 and 25.1, respectively).[27] The stability constants for the Fe(III) complexes of the X-Sal-AHA chelates are between those found for the AHA plus hydroxamate-containing siderophores, aerobactin, aquachelin C, and marinobactin E (log K = 27.6, 31.3, and 31.8, respectively) and the catecholate-containing siderophores petrobactin, enterobactin, and alterobactin A (log K = 43, 49, and 51, respectively).[3,4,28] They are significantly higher than the bis(AHA)-containing siderophores vibrioferrin and rhizoferrin (log K = 24.0 and 25.3, respectively) which do not have either hydroxamate or catecholate coordinating groups.[6] The high stability constants for the $[Fe_3(X\text{-Sal-AHA})_3(\mu_3\text{-OR})]^-$ complexes likely come from two contributions. First, the phenolate group has a high affinity for Fe(III), with the more electron donating ring substituents giving stronger binding than the electron-withdrawing substituents. Second, the formation of the $Fe(III)_3$ cluster with a μ_3-OR bridge, three μ_2-OR bridges, and the remaining coordinating groups from a given chelate spanning two metals provides extra stability to the complex, a sort of "super chelate effect".

The UV/visible absorption spectra of the five $[Fe_3(X\text{-Sal-AHA})_3(\mu_3\text{-OR})]^-$ complexes in methanol are shown in Figure 3. Each has a visible transition maximizing between 450 and 550 nm. This is tentatively assigned as a phenolate-to-Fe(III) ligand-to-metal charge transfer (LMCT), as LMCT transitions from phenolates tend to be found at lower energy than from most other N- or O-donor ligands. The trend in energy of this transition through the series of derivatives is consistent with this assignment, with the more electron withdrawing substituents lowering the energy of the phenolate-centered orbitals and thus producing higher energy LMCT transitions than the more electron donating substituents. Most of the intensity associated with this feature

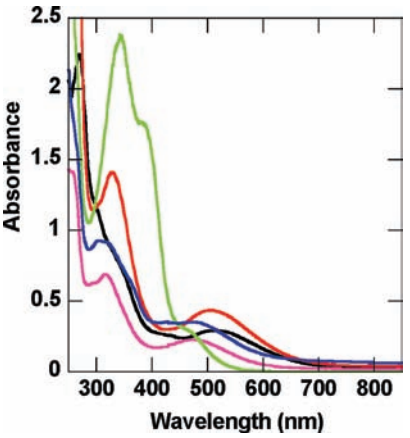

Figure 3. UV/visible absorption spectra of the Fe(III) complexes of the five X-Sal-AHA derivatives, approximately 0.1 mM in methanol: X = 5-NO_2 (green), 3,5-diCl (blue), H (purple), 3,5-di-*t*-Bu (red), 3-OCH_3 (black).

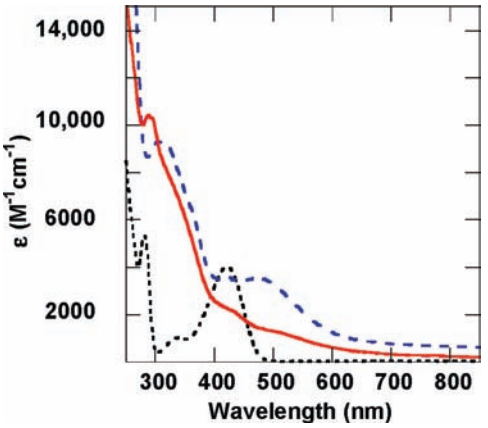

Figure 4. Comparison of the UV/visible absorption spectra of $Na[Fe_3(3,5\text{-diCl-Sal-AHA})_3(\mu_3\text{-OCH}_3)]$ (blue dashed line) before irradiation and the photolysis product after irradiation (red solid line), both in methanol under aerobic conditions. The spectrum of the free ligand is the black dotted line.

is lost upon irradiation, as shown for the 3,5-diCl derivative in Figure 4. Several intense features are observed for each derivative in the range of 250−450 nm. The α-hydroxy acid-to-Fe(III) LMCT transitions that are responsible for the photochemical activity are expected to be in this region. The analogous transition is found around 300 nm in marine siderophores[1,4] and between 350 and 400 nm in Fe(III) complexes of smaller AHA ligands.[29] This is the same region where multiple transitions are found in the spectra of the free ligands (see Supporting Information). While there is an increase in intensity of the absorbance in this region of the spectra upon iron binding, and a subsequent decrease upon irradiation of the Fe complexes (Figure 4), the congestion and shifting of bands in this region put specific assignment of the AHA-to-Fe(III) LMCT transition outside the scope of this paper.

The photolysis reaction can be monitored from the point of view of both chelate ligand cleavage and iron reduction. The intact complexes have rich circular dichroism (CD) spectra because of the chirality of the chelates (see Figure 5). Upon

(25) Taylor, S. W.; Luther, G. W., III; Waite, J. H. *Inorg. Chem.* **1994**, *33*, 5819–5824.
(26) Martell, A. E.; Smith, R. M. *Critical stability constants*; Plenum Press: New York, 1977; Vol. *3*.
(27) Martell, A. E. *Critical stability constants*; Plenum Press: New York, 1974; Vol. *1*.
(28) Zhang, G.; Amin, S. A.; Kupper, F. C.; Holt, P. D.; Carrano, C. J.; Butler, A. *Inorg. Chem.* **2009**, *48*, 11466–11473.
(29) Sen Gupta, K. K.; Chatterjee, A. K. *J. Inorg. Nucl. Chem.* **1976**, *38*, 875–876.

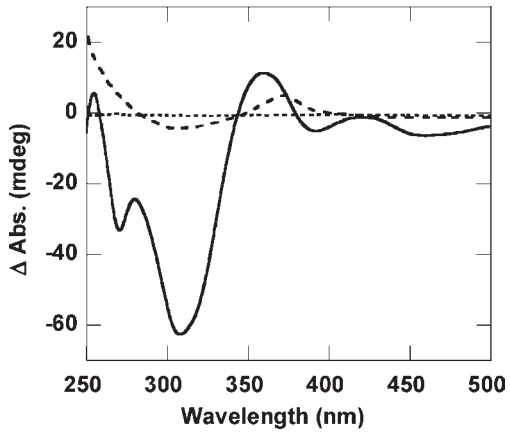

Figure 5. Circular dichroism spectra of $Na[Fe_3(3,5\text{-diCl-Sal-AHA})_3(\mu_3\text{-}OCH_3)]$ in methanol: dark control (solid line), aerobic irradiation (dotted line), anaerobic irradiation (dashed line).

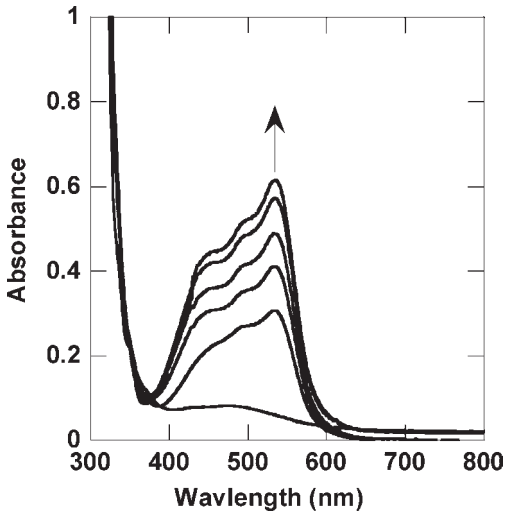

Figure 6. UV/visible spectral changes over time upon irradiation in air of 0.02 mM $Na[Fe_3(3,5\text{-diCl-Sal-AHA})_3(\mu_3\text{-}OCH_3)]$ in the presence of 0.2 mM BPDS in methanol. Spectra, in order of increasing intensity, are as follows: dark control, and 5, 10, 23, 45, and 150 min of irradiation in sunlight.

irradiation in air, the CD spectrum disappears, while under anaerobic conditions, the CD spectrum does not disappear completely upon irradiation. Rather, it is replaced by a different, less intense spectrum. The structures of the photolysis products of the chelates reported here have not yet been determined, but remain under study. However, photolysis of the Fe(III) complex of the AHA-containing citrate, an Fe_2L_2 dimer, results in decarboxylation of the AHA in one citrate to give the ketone for every two Fe reductions.[8,30] Some of the AHA-containing marine siderophores, such as petrobactin, aerobactin, and vibrioferrin undergo a similar 2:1 Fe reduction/ligand decarboxylation reaction, while others like the aquachelins undergo more extensive ligand cleavage that also results in loss of the AHA group.[1,2,4,6] Loss of the CD signal upon irradiation of the Fe(III)(X-Sal-AHA) complexes is most likely due to loss of the AHA group in these reactions as well. The complete loss of the signal under aerobic but not anaerobic conditions suggests that in the absence of O_2, all of the Fe(III) is reduced before an equal amount of chelate ligand is oxidized. Some of the intact AHA chelate would remain, perhaps coordinated to Fe(II), giving a different CD spectrum. In contrast, under aerobic conditions, the Fe(II) is reoxidized by O_2 to complete the ligand photolysis and eliminate the CD signal. This is consistent with the 2:1 Fe reduction to ligand oxidation stoichiometry for the decarboxylation reactions noted above. The structure of the $[Fe_3(X\text{-Sal-AHA})_3(OR)]^-$ complexes, in which each ligand is coordinated to two irons, may facilitate a reaction with this Fe:L electron stoichiometry. Neither the CD spectrum nor the NMR spectrum of the metal-free chelate shows significant change upon aerobic irradiation for 3 h in sunlight (see Supporting Information), confirming that the free chelate is not itself photoactive, as expected based on prior work.[7]

Reduction of iron upon irradiation can be monitored by the addition of bathophenanthroline disulfonate (BPDS) to the solution. This bidentate phenanthroline derivative forms a strongly absorbing chromophore with Fe(II), but shows little absorbance in the presence of Fe(III). The absorbance at 535 nm can be used to determine the concentration of Fe(II) transferred from the X-Sal-AHA chelate upon irradiation, modeling iron reduction and transfer in the marine siderophores. The spectral change over time during irradiation of $Na[Fe_3(3,5\text{-diCl-Sal-AHA})_3(\mu_3\text{-}OCH_3)]$ in the presence of BPDS is shown in Figure 6. For a given derivative, the rate of photolysis in the presence of BPDS is independent of the presence or absence of air. However, if BPDS is not added until after irradiation to determine the amount of Fe(II) produced, far less absorption is observed at 535 nm in the aerobic case than the anaerobic case. This suggests that BPDS offers some protection to the Fe(II) from reoxidation to Fe(III) by air. All five derivatives produce $Fe(II)(BPDS)_3$ corresponding to 50−60% of the total Fe after 2−3 h of irradiation. In analogous studies reported on Fe(II) transfer upon irradiation of the siderophore Aquachelin, about 70% of the iron as $Fe(II)(BPDS)_3$ is observed.[1] The observation of less than 100% of the iron in this form is likely due to competition between the photolysis product of the chelate (which maintains some chelating ability) and the BPDS, and possibly some percentage of the iron being reoxidized by air even in the presence of BPDS. In contrast to the siderophore ferrioxamine B, where formation of a ternary complex with BPDS is necessary to facilitate the chemical reduction of Fe,[31] the presence of BPDS is clearly not needed for the photochemical reduction of iron in the complexes with X-Sal-AHA, but only stabilizes the resulting Fe(II) in air once the photoreduction occurs.

The rate of Fe(II) production differs for the different derivatives as shown by comparison of the absorbance at 535 nm (Abs_{535}) versus irradiation time in Figure 7A. It is clear that the electron donor ability of the phenolate group, and thus the electron density on the iron, affects the observed rate of photolysis of the $Fe_3(X\text{-Sal-AHA})_3$ complexes. Figure 7B shows a plot of Abs_{535} after 10 min of irradiation versus the Hammett σ^+ parameter for each derivative. This time point was chosen as it is within the region of approximately linear increase in absorption for all five derivatives, while providing time for sufficient progress in the slower ones. The plot is linear ($R = 0.992$) with a positive slope (ρ).

(30) Shweky, I.; Bino, A.; Goldberg, D. P.; Lippard, S. J. *Inorg. Chem.* **1994**, *33*, 5161–5162.

(31) Mies, K. A.; Wirgau, J. I.; Crumbliss, A. L. *BioMetals* **2006**, *19*, 115–126.

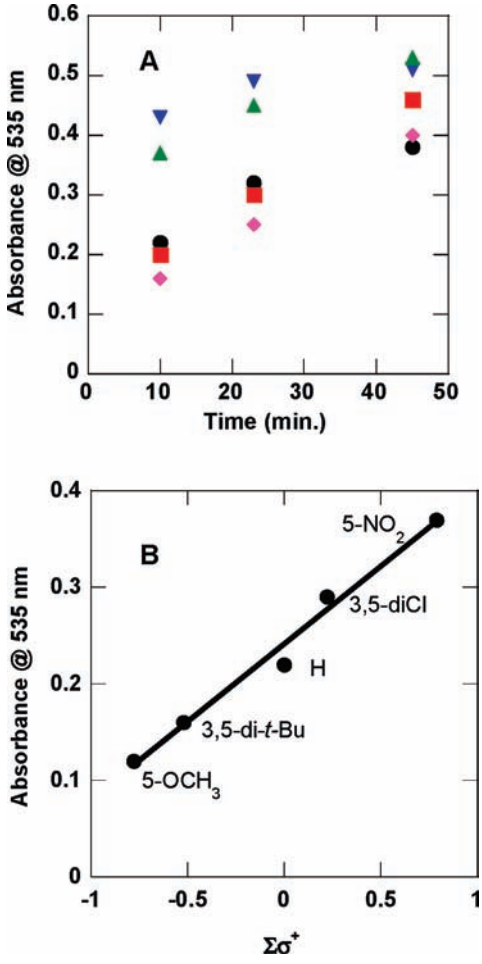

Figure 7. (A) Absorption at 535 nm versus time during side-by-side irradiation of the Fe(III) complexes of the five X-Sal-AHA derivatives in the presence of BPDS: X = 5-NO_2, blue inverted triangles; X = 3,5-diCl, green triangles; X = H, black circles; X = 3,5-di-*t*-Bu, red squares; X = 3-OCH_3, purple diamonds. (B) Plot of the 10 min data points from (A) versus the sum of the Hammett σ^+ parameters corresponding to the phenolate ring substituents, X. The equation for the best fit line is Abs = $0.24 + 0.16\Sigma\sigma^+$, $R = 0.992$.

The positive slope is not surprising, since the more electron withdrawing groups are expected to favor the Fe(II) product relative to the more electron donating groups.

In summary, this paper describes a series of new chelate ligands that are designed to bind Fe(III) and to release it upon irradiation as Fe(II). Each of the new chelates contributes phenolate and imine coordinating groups in addition to the bidentate α-hydroxy acid moiety. The chelate structure results in Fe(III) complexes characterized by a poly(alkoxo)-bridged cluster with very high stability constants. Each ligand in the trimeric complexes spans two irons, with the alkoxo oxygen from the AHA moiety bridging the irons. In addition, an unusual μ_3-methoxy group caps the iron atoms. Despite the similarity in structures of the series of Fe(III) complexes varying only in the phenolate ring substituents, this variation results in significant differences in the bulk photolysis rates as determined by the relative rates of Fe(II) transfer to the BPDS receptor upon irradiation. These studies present the first systematically varied series of mixed-donor, α-hydroxy acid-containing chelates and demonstrate that the AHA functional group has great potential for development of tight iron-binding and photorelease agents. They also show that straightforward modification of an ancillary donor group in AHA-containing chelates can be used to tune the kinetics of Fe(II) release. Modulation of other properties of these molecules by ancillary functional group modification, including the action spectrum, is being explored. This work is being extended to examine the effect of chelate backbone structure and ancillary functional group replacement on tuning the AHA-containing chelates for application-specific metal binding and release in response to a light stimulus.

Acknowledgment. The authors thank Prof. Apryll Stalcup (University of Cincinnati) for use of her circular dichroism spectrophotometer and her student, Floyd Stanley, for assistance with the CD experiments. Funding for the SMART6000 diffractometer was through NSF-MRI Grant CHE-0215950.

Supporting Information Available: NMR data for the five chelates; mass spectrometry data for the five Fe(III) complexes; comparison of UV/visible absorption spectra for the ligand, Fe(III) complex, and photolysis product for each of the four derivatives not shown in the main text; cyclic voltammograms of the Fe(III) complexes; CD spectra of 3,5-diCl-Sal-AHA before and after irradiation; and complete crystallographic details and CIF files for $Na[Fe_3(3,5\text{-diCl-Sal-AHA})_3(OCH_3)]\cdot 3.5\ H_2O$ and (*S*)-(-)-4-amino-2-hydroxy-butyric acid (30 pages). This material is available free of charge via the Internet at http://pubs.acs.org.